

# Stability Investigation of Extracted Lignins from Bagasse, Coconut Husk, Rice Straw, and Corn Stover: Kinetic and Thermodynamic Aspects

Tirapote Rattana-amron<sup>1,2,\*</sup>, Navadol Laosiripojana<sup>1,3</sup>, and Wiyong Kangwansupamonkon<sup>2,3</sup>

<sup>1</sup>The Joint Graduate School of Energy and Environment, King Mongkut's University of Technology Thonburi, Bangkok 10140, Thailand

<sup>2</sup>National Nanotechnology Center (NANOTEC), National Science and Technology Development Agency (NSTDA), Pathum Thani 12120, Thailand

<sup>3</sup>AFRS(T), The Royal Society of Thailand, Sanam Sueapa, Dusit, Bangkok 10300, Thailand

## ABSTRACT

The influence of different biomasses on lignin extraction impacts the thermal stability of lignin. Four extracted lignins from the soda pulping process were prepared from agricultural wastes, including bagasse, coconut husk, rice straw and corn stover. Kinetic and thermodynamic analyses were utilized to compare and investigate the thermal-oxidative stability behavior of all lignins. Experiments were conducted using the non-isothermal method for four heating rates with a thermogravimetric analyzer. The Friedman, FWO, KAS and Starink kinetic methods were used to investigate the oxidative kinetics of lignins. Thermodynamic parameters involving enthalpy ( $\Delta H$ ), Gibbs free energy ( $\Delta G$ ) and entropy ( $\Delta S$ ) were considered for observing thermal characteristics. Thermal degradation of lignin consists of three consecutive regimes: moisture content, lignin degradation and decomposition of residues. All kinetic models showed average activation energies between 132.89 and 144.52 kJ/mol, 109.75 and 121.72 kJ/mol, 156.62 and 167.98 kJ/mol and 160.11 and 171.64 kJ/mol for BG, CH, RS and CS, respectively. The coefficient of determination revealed that all models are promising kinetic methods for calculating kinetic parameters. The fluctuation of kinetic and thermodynamic parameters showed that the thermal oxidative degradation of lignin was a complicated mechanism. The conversion process corresponds to a non-spontaneous endothermic reaction. The results provide valuable information to deeply understand the thermochemical conversion for characterizing the thermal stability of lignins.

**Keyword:** Soda lignin extraction/ Agricultural wastes/ Thermal oxidative degradation/ Kinetic and thermodynamic

## 1. INTRODUCTION

The production of agricultural waste increases as a result of the growing worldwide population and rising demand for agricultural products [1]. Agriculture is the most important sector to drive the Thai economy with high domestic and overseas demands for rice, sugar, coconut and corn [2]. The production of these agricultural wastes is created by the harvesting operations and the food processing industries. Currently, burning is an efficient method for removing excessive residues due to its inexpensive, rapid and uncomplicated approach [3]. The combustion process releases particulate matter, black carbon and greenhouse gases (GHGs) into the atmosphere, affecting air pollution, climate change and human health. Therefore, managing agricultural residues illustrates the greatest challenge for waste management in agricultural countries. Converting agricultural waste into high value products, including polysaccharides (cellulose and hemicelluloses) and lignin as aromatic polymers, remains economical, sustainable and advantageous for humans and the environment [4].

Lignin demonstrates excellent antioxidant properties; it has been promisingly utilized in many applications, such as film fabrication, thermo-oxidation stabilizers, and polymer additives [5]. Thermal stability and decomposition profiles are normally evaluated via thermal gravimetric analysis (TGA). But the results of TGA thermograms cannot disclose the reaction mechanisms during thermal degradation.

---

\*Corresponding Author: Tirapote Rattana-amron  
E-mail address: tirapote@nanotec.or.th

Kinetic and thermodynamic analyses provide beneficial information through kinetic and thermodynamic parameters for revealing the mechanisms and thermal degradation behavior. Kinetic analysis focuses on the determination of kinetic parameters such as activation energy ( $E$ ) and pre-exponential factor ( $A$ ). The obtained kinetic parameters are calculated from different kinetic models. Model-free methods are generally used for predicting kinetic parameters. Model-free techniques have isoconversional bases. This method works well for uncovering intricate chemical reaction processes that involve multiple elementary steps in their mechanisms. The rate of reaction is related to temperature and the kinetic parameters are assessed at a constant conversion degree [6]. Model-free approaches can be categorized into two main categories: differential and integral kinetic methods. The differential kinetic methods such as Friedman produce the most precise kinetic findings, but they have a defect in that noise from data amplification through numerical differentiation may influence accuracy [7]. The methods of studying material stability that have gained widespread acceptance include the integral isoconversional kinetics of Flynn-Wall-Ozawa (FWO), Kissinger-Akahira-Sunose (KAS), and Starink. However, because of the Arrhenius integral's oversimplified estimation and the activation energy constant assumption used in their derivation, these kinetic techniques would lead to systematic calculation errors [8]. Thermodynamic analysis is used to forecast the possibility of a chemical or physical reaction, which includes occurring on its own initiative, based on the distribution of energy contained in reactants and products. Thermodynamic parameters involving enthalpy ( $\Delta H$ ), Gibbs free energy ( $\Delta G$ ) and entropy ( $\Delta S$ ) are utilized to describe spontaneous reactions, absorbed or released energy, stability determination as well as the degree of disorder [9]. The study of oxidative degradation kinetics in lignin in terms of characteristics, kinetic mechanism, thermodynamic analysis and comparison between different kinetic methods is limited and not well understood.

Determining the thermal oxidative stability of lignins derived from bagasse, coconut husk, rice straw, and maize stover was the primary objective of this study. Kissinger-Akahira-Sunose (KAS), Flynn-Wall-Ozawa (FWO), Friedman, and Starink models' kinetic parameters were predicted using the TGA and DTG results of soda lignin degradation, which were based on the kinetic analysis. Activation energy data were used to determine thermodynamic parameters such as entropy ( $\Delta S$ ), Gibbs free energy ( $\Delta G$ ), and enthalpy ( $\Delta H$ ). The results of thermodynamic and kinetic assessments included comparisons of various kinetic techniques, kinetic mechanisms, and features of thermal degradation. The variance of lignin compounds in these various biomasses was also seen by analyzing a number of other factors, including chemical composition, molecular structure, and glass transition temperature.

## 2. METHODOLOGY

### 2.1 *Materials and methods*

Four agricultural residues were used to extract the soda lignin. Coconut husk (CH), rice straw (RS) and corn stover (CS) were collected from local fields in Thailand and bagasse (BG) was obtained from the sugar factory in the central region. Dry samples were carried out in an oven at 50 °C for 4 days to remove the moisture content and crushed with a laboratory grinder mixture. The particle size of lignin samples was controlled to less than 3 mm with a sieve and stored at room temperature in zip lock plastic bag.

### 2.2 *Lignin dissolution and precipitation*

Soda lignin was prepared by the soda pulping process utilizing an alkaline hydrolysis based on sodium hydroxide (NaOH). Four samples were mixed with 3% (w/v) of NaOH solution at a ratio of solid to liquid of 1:12 (w/v). The reaction temperature was adopted at 121 °C for 1 h for reaction time and the pressure was kept at 15 psi. Next, fibers and excess pulp residues were separated by vacuum filtration

several times. Black liquor had a high alkali content, showing a pH of approximately 11. The precipitation of lignin was carried out by adding 20% (v/v) of sulfuric acid to black liquor under magnetic stirring. The amount of sulfuric acid in black liquor was controlled by reaching pH 2 and samples were set for 1 day at 25 °C. Subsequently, precipitated lignin was filtrated to remove excess water with a centrifugation speed of 4000 rpm and a time of 15 minutes. The washing process with hot water at 60 °C was adopted many times to neutralize the pH of lignin. Finally, all soda lignins were dried for 5 days in an oven at 55 °C to reduce moisture and then milled to powder. Extraction processes are expressed in Figure 1.

### 2.3 Thermogravimetric analysis (TGA)

The thermal oxidative degradation characteristics and kinetic analysis of soda lignins were tested by a thermogravimetric analyzer (TGA/DSC Mettler-Toledo). The weight loss profile was a function of mass change under increasing temperatures. Approximately 10 mg of lignin was allowed to stabilize at 25 °C in an alumina crucible. Thermal oxidative degradation behavior was achieved at temperatures from 25 to 800 °C under heating rates of 5, 10, 20 and 30 °C/min. TGA results are not only used to describe data on weight loss but also to determine kinetic parameters. To ensure reproducibility, a minimum of three replications were conducted.

### 2.4 Kinetics analysis

Evaluating the reaction mechanism of lignin degradation becomes more difficult because of the complicated chemical composition. The model-free isoconversional methods, including Friedman, Flynn-Wall-Ozawa (FWO), Kissinger-Akahira-Sunose (KAS) and Starink were employed for approximating the activation energy and pre-exponential factor. Generally, when biomass is thermally degraded, a number of parallel and simultaneous processes take place and the reaction is described in Eq. (1).



The reaction rate is dominated by the conversion function  $f(\alpha)$  and can be defined by the following equation:

$$\frac{d\alpha}{dt} = A e^{\left(\frac{E}{RT}\right)} f(\alpha) \quad (2)$$

The terms of  $E$ ,  $A$ ,  $R$ ,  $T$  and  $t$  represent the activation energy of reaction, pre-exponential/frequency factor, gas constant, absolute temperature and reaction time, respectively. The instantaneous conversion ratio ( $\alpha$ ) of biomass can be expressed as:

$$\alpha = \frac{m_i - m_t}{m_i - m_f} \quad (3)$$

Where  $m_t$  is the mass at a considered time,  $m_i$  and  $m_f$  designate initial mass and final mass. A constant heating rate ( $\beta = dT/dt$ ) for non-isothermal condition is added to Eq. (2), the new function can be generated as follows:

$$\frac{d\alpha}{dT} = \frac{E}{\beta} e^{\left(\frac{E}{RT}\right)} f(\alpha) \quad (4)$$

Based on Eq. (4), rearranging and integrating can be expressed as:

$$g(\alpha) = \int_0^\alpha \frac{d\alpha}{f(\alpha)} = \frac{A}{\beta} \int_{T_0}^T e^{\left(\frac{E}{RT}\right)} dT = \frac{AE}{\beta R} \int_x^\alpha \frac{e^{-x}}{x^2} dx = \frac{AE}{\beta R} p(x) \quad (5)$$

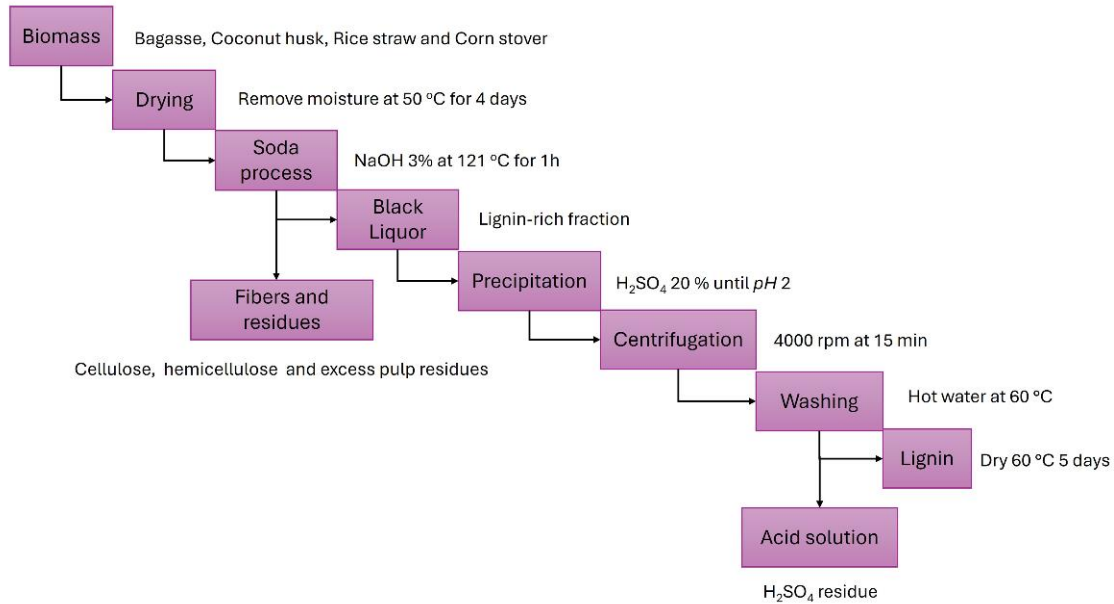


Figure 1. Schematic diagram of lignin extraction from agricultural residues.

The term  $g(\alpha)$  is the reaction model function of integral form and  $p(x)$  represents the Arrhenius integral/temperature integral function. It has no analytical solution except utilizing different approximation approaches for determination [10].

#### 2.4.1. Friedman method

The assumption of Friedman method proposes the conversion function  $f(\alpha)$  will be constant. This indicates that thermal degradation depends on the mass loss rate but is not influenced by temperature [11]. By taking natural logarithm of Eq. (4), Friedman differential isoconversional method can be obtained [12]:

$$\ln\left(\frac{d\alpha}{dt}\right) = \ln\left[\beta\left(\frac{d\alpha}{dt}\right)\right] = \ln A + \ln(f(\alpha)) - \frac{E}{RT} \quad (6)$$

Plotting  $\ln(d\alpha/dt)$  against  $1/T$  for a specified conversion value provides the slope and  $-E/R$  can be evaluated from a slope.

#### 2.4.2. Flynn-wall-ozawa (FWO) method

FWO applied Doyle's approximation at  $\ln p(x) \cong -5.3305 - 1.051x$ . Based on the method developed by FWO, it can be expressed as follows [13,14]:

$$\ln(\beta) = \ln\left(\frac{AE}{g(\alpha)R}\right) - 5.3305 - 1.0516\left(\frac{E}{RT}\right) \quad (7)$$

Since  $\ln(AE/g(\alpha)R)$  keeps constant, the relationship of  $\ln(\beta)$  relates to  $1/T$  to offer a linear function. The  $E$  can be determined by the slope of this line  $-1.0516 (E/RT)$ .

#### 2.4.3. Kissinger -Akahira -Sunose (KAS) method

This integral isoconversional method is commonly used in the comparative kinetic study of several materials. The assumption of KAS method fixed the value of the conversion and applied Doyle approximation for substituting the temperature integral function [15]. The general equation of KAS is presented in Eq. (8) [16,17].

$$\ln\left(\frac{\beta}{T^2}\right) = \ln\left(\frac{AR}{Eg(\alpha)}\right) - \frac{E}{RT} \quad (8)$$

Similar as FWO method, the plot of  $\ln(\beta/T^2)$  versus  $1/T$  provides a linear function. The slope of this line equals to  $-E/RT$ .

#### 2.4.4. Starink method

Starink considered both FWO and KAS kinetic approaches and proposed a more accurate kinetic method by combining both FWO and KAS with correct approximation [18,19]. Starink method can be expressed as follows [20]:

$$A = \ln\left(\frac{\beta}{T^{1.92}}\right) = \ln\left(\frac{AR^{0.92}}{g(\alpha)E^{0.92}}\right) - 1.0008\left(\frac{E}{RT}\right) - 0.312 \quad (9)$$

The slope of  $\ln(\beta/T^{1.92})$  versus  $1/T$  gives a linear function and  $E$  can be achieved from the slope of  $-1.0008(E/RT)$ .

### 2.5 Thermodynamic analysis

Kinetic information from Friedman, FWO, KAS and Starink kinetic models is utilized to estimate the parameters of thermodynamic in various extracted lignins. The frequency factor can be obtained from Eq. (10). Thermodynamic determinations, involving the changes of enthalpy ( $\Delta H$ ), Gibbs free energy ( $\Delta G$ ) and entropy ( $\Delta S$ ) are presented in Eq. (11) to (12) [21]:

$$A = \left[ \beta E \exp\left(\frac{E}{RT_p}\right) \right] \frac{1}{RT_p^2} \quad (10)$$

$$\Delta H = E - RT \quad (11)$$

$$\Delta G = E - RT_p \ln\left(\frac{KT_p}{hA}\right) \quad (12)$$

$$\Delta S = \frac{(\Delta H - \Delta G)}{T_p} \quad (13)$$

Where  $K$  represents the Boltzmann constant of  $1.381 \times 10^{-23}$  (J/K),  $h$  corresponds to the Planck constant of  $6.626 \times 10^{-34}$  (J·s) and  $T_p$  denotes the temperature (K) of the DTG peak.

### 3. RESULTS AND DISCUSSION

#### 3.1 Yields of lignin extraction

Four different biomasses of bagasse (BG), coconut husk (CH), rice straw (RS) and corn stover (CS) were selected to extract lignin through soda pulping. The percentage yield of lignin from different sources was determined by the gravimetric method and the results are presented in Table 1. CH yielded the highest lignin level of 38.51%, followed by BG, RS and CS with yields of 31.34%, 19.37% and 15.85%, respectively. Regarding the separation of fiber in black liquor, rapid clogging was found in rice straw and corn stover using filtration. However, this problem could not be observed in bagasse and coconut husk.

#### 3.2 Thermogravimetric analysis

The thermogravimetry (TG) and derivative thermogravimetry (DTG) representing mass loss and degradation rate with respect to temperature under the air are shown in Figure 2. The first regime under 100 °C could be attributed to moisture evaporation, which was relatively small (4-5%). The second regime described the major degradation stage of lignin. It was observed predominantly in the range of 180–400 °C. This can be assigned to the degradation of lignin showing dehydrogenation of the hydroxyl group of benzyl and the fragmentation of  $\alpha$ -O-4 and  $\beta$ -O-4 ether bonds at inter-unit linkages [22]. The third regime of lignin degradation occurred at a temperature above 400 °C. This segment occurred slowly to form char and various volatiles (H<sub>2</sub>, CO<sub>2</sub>, CH<sub>4</sub> and hydrocarbons) were produced and finalized with char combustion in the presence of oxygen [23-25]. The ash residue could be observed at the final stage of thermal oxidative degradation. The amount of ash from RS and CS samples was higher than that from BG and CH around 1–2%. The formation of these inorganic salts and mineral components influences

The amount of lignin ash and its thermochemical properties [26]. According to this study, low ash formation was observed for all four lignin samples. This indicated that the washing process in this study was effective enough to remove contaminants. The thermal degradation of lignin is obviously controlled by variations in heating rates. As shown in Table 2, shifting to a higher temperature was evident with increasing heating rates from 5 to 40 °C/min. The shifting temperature is attributed to the effect of heat transfer limitations. At high heating rates, samples cannot maintain a homogeneity of temperature between core and surface. It extends the temperature gradients and results in faster devolatilization [27-29]. The effect of different heating rates is also significant on the yield of residue (ash or char) at the end of thermal degradation. Results showed that the residue after thermal degradation using heating rates of 5, 10 and 20 °C/min yielded ash, while increasing the heating rate up to 40 °C/min only char was observed at the end of the degradation process. Thermal oxidative degradation of lignin requires a period to complete the degradation step for converting char to ash. At the highest heating rate of 40 °C/min cannot provide sufficient time to complete the combustion process [30].

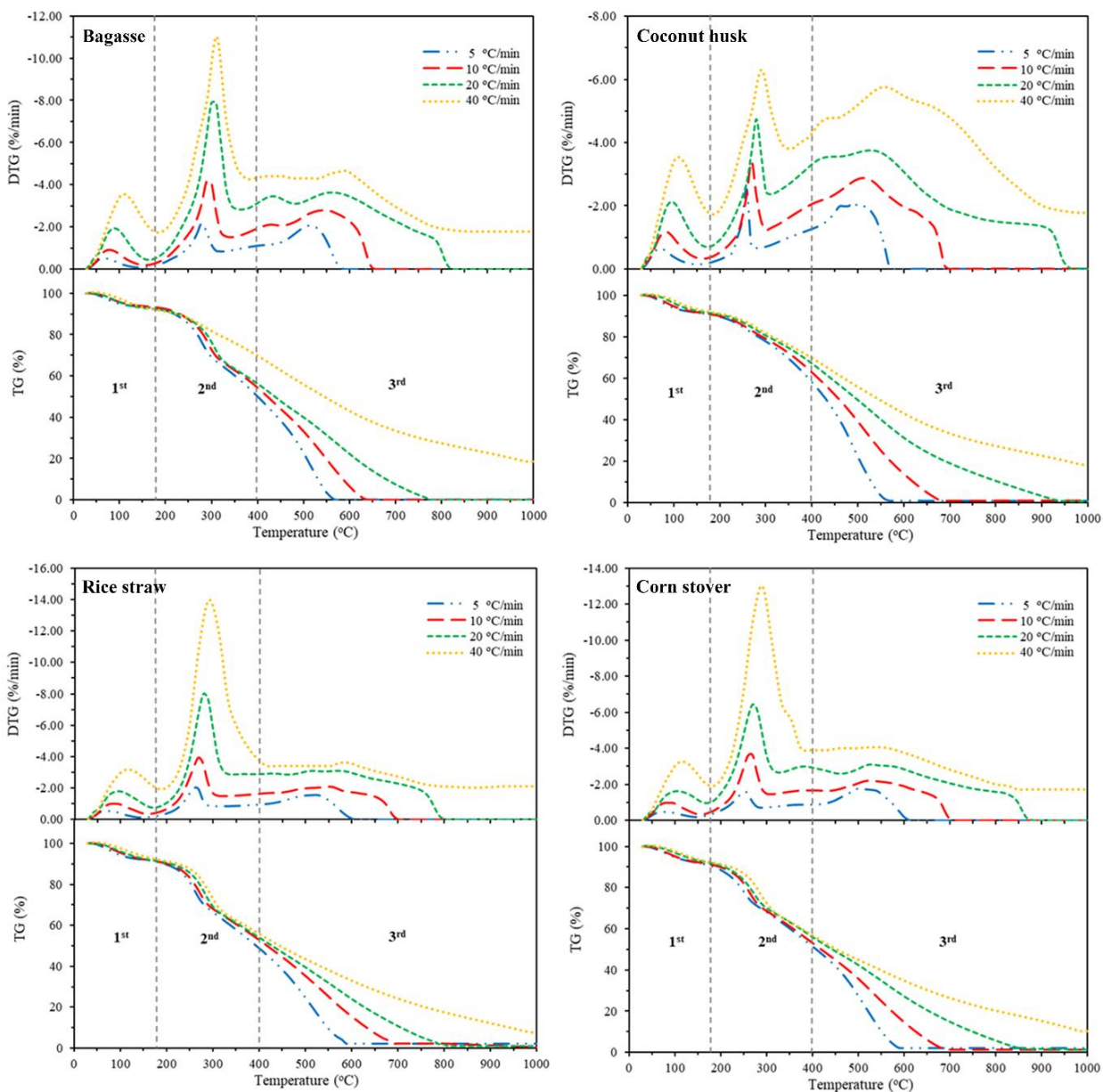


**Figure 2.** TG and DTG profiles of four different lignins.

### 3.3 Kinetic analysis

The linear regression plots of four model-free methods for all lignins are shown in Figure 3. The average activation energy ( $E$ ) values are summarized in Figure 4. The linear correlation coefficient ( $R^2$ ) is typically used to compare several kinetic models with respect to the acceptable accuracy of the results. High  $R^2$  signifies the optimal kinetic model with experimental data. Moreover, the causes of poor fits may be due to the high heterogeneous secondary formation of char and ash residues [8,31]. The results of thermal degradation in BG, CH, RS and CS lignins in this study show in Table 3 that high  $R^2$  values were apparent using the Friedman, FWO, KAS and Starink methods. Therefore, all kinetic models were considered promising methods to apply for determining the stability of lignin from different biomasses at a high level of acceptable accuracy.

The combination of Friedman, FWO, KAS and Starink kinetic models to determine the average  $E$  values is shown in Figure 4. By comparing the individual biomasses, the horizontal lines represented the means of the  $E$  throughout the whole degradation process. These lines indicated that extracted lignin from CS (164.05 kJ/mol) and RS (159.96 kJ/mol) had higher activation energies than BG (136.24 kJ/mol) and CH (114.01 kJ/mol). With an increase in conversion, the degradation behavior of all lignin samples could be observed to indicate that high energy requirements occurred in the beginning and decreased continuously until the end of the degradation process. The thermal degradation profiles of combination kinetic models also confirmed that the thermal oxidative degradation of soda lignin was the result of multiple reaction systems.

The statistical analysis for comparing the variances of four kinetic models showed that at the  $p = 0.05$  level of significance, the critical  $F$ -distribution was adapted with a 95% confidence interval and correlated with the right tail area. The error degree of freedom connected with the number of observations was 64, whereas the treatment degree of freedom related to the number of kinetic models was 3. The critical  $F$ -distribution ( $F_{(p=0.05, 3, 64)}$ ) was 2.7481 and the  $F$ -test results of BG (0.1188), CH (0.1634), RS (0.0717) and CS (0.0575) were lower than the critical value, accepting them for analysis of statistical data. It can be stated that there is no difference in the average of these four kinetic methods within the test population. The  $A$  results of soda lignins from four different biomasses are exhibited in Table 1. The  $A$  value of CH lignin degradation at  $\alpha = 0.2$  was  $10^{18} \text{ s}^{-1}$ , while BG, RS and CS lignins were degraded at different  $\alpha$  of 0.35 and showed  $A$  values between  $10^{24}$  and  $10^{32} \text{ s}^{-1}$ . The value of  $A$  is less than  $10^9 \text{ s}^{-1}$ , indicating a surface-control reaction but the  $A$  value is higher than  $10^9 \text{ s}^{-1}$ , meaning that the reaction is independent of surface area [30,32].

### 3.4 Thermodynamic analysis

According to thermodynamic analysis, kinetic parameters ( $E$  and  $A$ ) of lignin degradation derived from four model-free methods were applied for thermodynamic parameter determination (Table 1). The  $\Delta H$  corresponds to a specific amount of heat energy that is necessary for degradation to break the heterometric linkages in the lignocellulosic biomass structure. The order of the average  $\Delta H$  from lower to higher is as follows: lignin CS > RS > BG > CH. A small  $\Delta H$  value is connected with the formation of the transition state at a lower energy barrier [33]. This means that CH lignin requires the lowest energy demand to degrade when compared with the others. The positive  $\Delta H$  were found during lignin degradation. This suggests that the energy required for the lignin thermal decomposition is a naturally endothermic process.

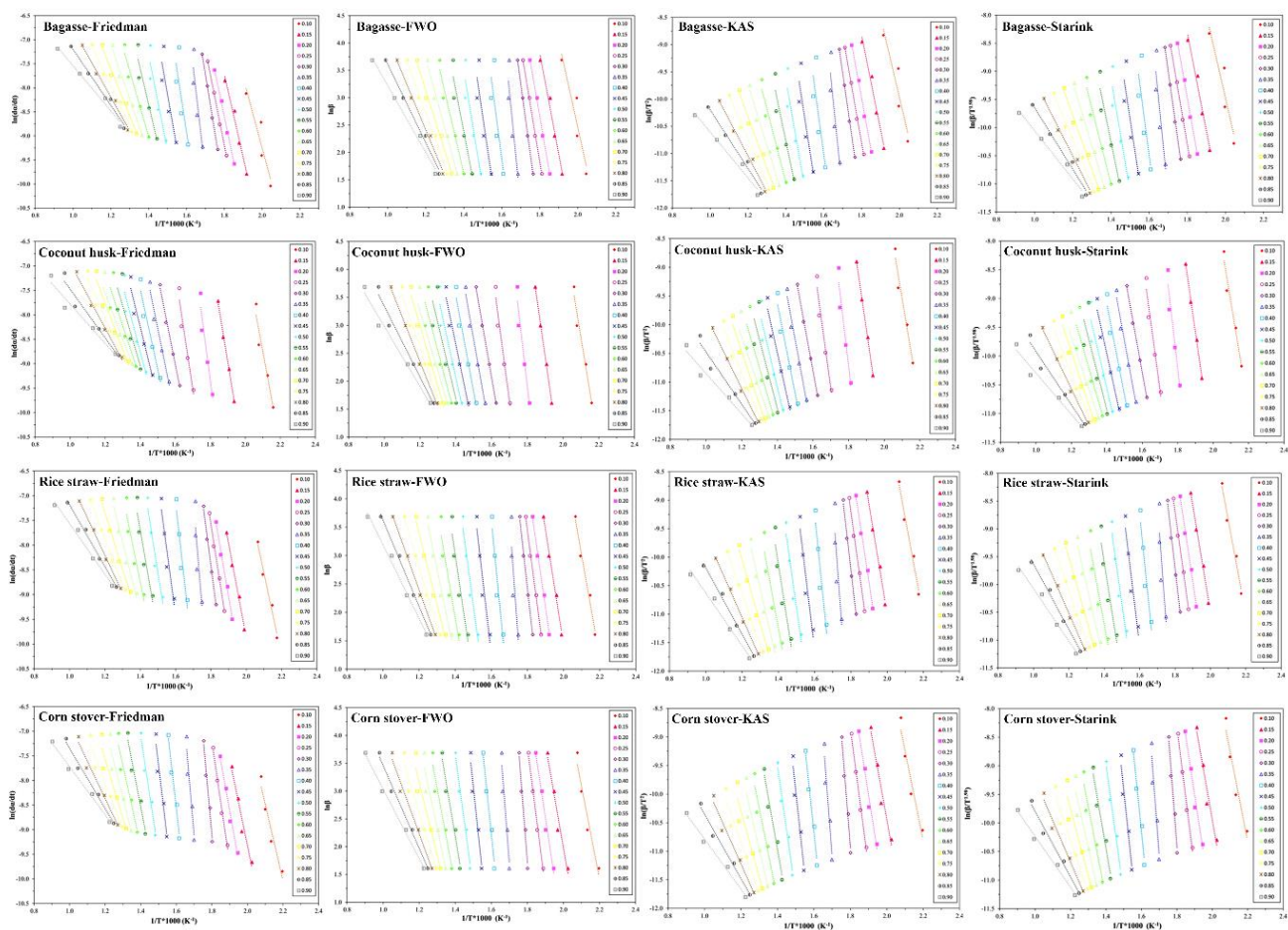


Figure 3. Linear regression plots of the Friedman, FWO, KAS and Starink models.

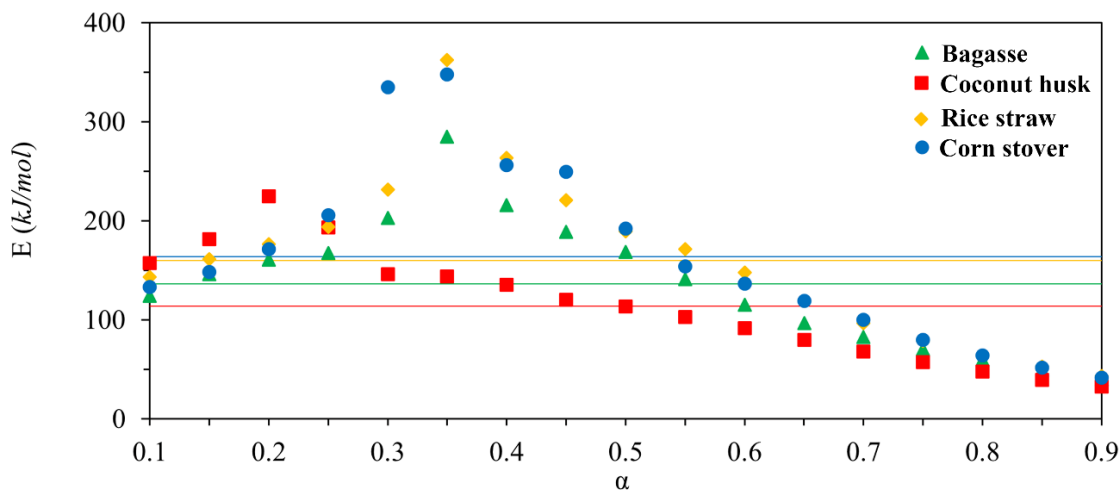


Figure 4. The average activation energies of Friedman, FWO, KAS and Starink models.

**Table 1.** Thermodynamic parameters of extracted lignins according to four model-free methods

$\alpha$	$A$ (s <sup>-1</sup> )				$\Delta H$ (kJ/mol)				$\Delta G$ (kJ/mol)				$\Delta S$ (J/mol)			
	Friedman	FWO	KAS	Starink	Friedman	FWO	KAS	Starink	Friedman	FWO	KAS	Starink	Friedman	FWO	KAS	Starink
<i>BG</i>																
0.10	1.5E+09	1.4E+10	2.2E+09	2.4E+09	116.00	126.24	117.82	118.16	163.53	163.14	163.46	163.44	-82.96	-64.41	-79.65	-79.04
0.15	1.8E+11	1.6E+12	2.3E+11	2.5E+11	138.10	148.14	139.19	139.55	162.73	162.40	162.69	162.68	-42.97	-24.90	-41.02	-40.37
0.20	4.6E+12	4.0E+13	5.4E+12	5.8E+12	153.01	162.98	153.74	154.11	162.26	161.96	162.23	162.22	-16.14	1.77	-14.83	-14.16
0.25	2.1E+13	1.8E+14	2.3E+13	2.5E+13	159.98	169.92	160.48	160.86	162.05	161.77	162.03	162.02	-3.61	14.22	-2.71	-2.03
0.30	4.5E+16	3.8E+17	4.8E+16	5.2E+16	195.67	205.59	195.95	196.33	161.12	160.89	161.11	161.10	60.30	78.01	60.80	61.49
0.35	2.0E+24	1.6E+25	1.9E+24	2.1E+24	277.87	287.79	277.78	278.18	159.48	159.31	159.48	159.47	206.63	224.21	206.45	207.16
0.40	7.8E+17	6.6E+18	6.9E+17	7.5E+17	208.93	218.88	208.34	208.76	160.81	160.59	160.82	160.81	83.99	101.72	82.93	83.68
0.45	2.3E+15	2.0E+16	1.8E+15	2.0E+15	181.81	191.83	180.80	181.24	161.46	161.21	163.22	161.47	35.52	53.44	30.69	34.51
0.50	3.3E+13	2.9E+14	2.4E+13	2.7E+13	162.10	172.21	160.72	161.18	161.99	161.71	162.03	162.01	0.20	18.32	-2.28	-1.45
0.55	9.1E+10	8.3E+11	6.2E+10	6.9E+10	134.88	145.09	133.15	133.62	162.84	162.50	162.90	162.88	-48.78	-30.38	-51.92	-51.06
0.60	3.2E+08	3.0E+09	2.0E+08	2.2E+08	108.88	119.23	106.78	107.28	163.82	163.40	163.91	163.89	-95.87	-77.10	-99.70	-98.80
0.65	5.3E+06	5.3E+07	3.1E+06	3.5E+06	90.28	100.77	87.84	88.35	164.67	164.17	164.79	164.77	-129.82	-110.65	-134.31	-133.36
0.70	2.4E+05	2.6E+06	1.3E+05	1.5E+05	76.35	86.98	73.60	74.14	165.42	164.84	165.59	165.56	-155.45	-135.88	-160.53	-159.54
0.75	1.6E+04	1.8E+05	8.3E+03	9.4E+03	64.26	75.04	61.22	61.77	166.19	165.50	166.41	166.37	-177.90	-157.88	-183.57	-182.54
0.80	1.5E+03	1.8E+04	7.2E+02	8.2E+02	53.75	64.69	50.42	50.99	166.98	166.16	167.26	167.21	-197.61	-177.09	-203.91	-202.83
0.85	1.5E+02	2.0E+03	6.6E+01	7.6E+01	43.69	54.83	40.03	40.62	167.88	166.89	168.25	168.19	-216.73	-195.58	-223.78	-222.64
0.90	1.8E+01	2.5E+02	6.7E+00	7.7E+00	34.35	45.74	30.28	30.90	168.90	167.68	169.42	169.34	-234.82	-212.81	-242.83	-241.60
Avg.	-	-	-	-	129.41	139.76	128.13	128.59	163.65	163.18	163.86	163.73	-	-	-	-
<i>CH</i>																
0.10	4.0E+12	4.8E+12	9.1E+11	9.7E+11	155.69	156.56	148.68	149.00	177.62	177.60	177.85	177.84	-38.27	-36.70	-50.91	-50.34
0.15	5.0E+14	1.0E+15	1.6E+14	1.8E+14	178.56	182.01	173.21	173.57	176.93	176.84	177.09	177.08	2.84	9.03	-6.76	-6.13
0.20	4.1E+18	1.0E+19	1.4E+18	1.5E+18	221.34	225.60	216.25	216.62	175.85	175.75	175.97	175.96	79.40	87.00	70.30	70.97
0.25	7.4E+15	1.3E+16	1.6E+15	1.8E+15	191.29	194.08	184.08	184.48	166.59	162.51	164.10	166.77	43.11	55.10	34.88	34.46
0.30	3.7E+11	6.3E+11	6.7E+10	7.3E+10	144.43	146.98	136.38	136.81	160.54	158.36	158.32	160.27	-28.12	-19.87	-38.28	-40.95
0.35	1.8E+11	4.9E+11	4.7E+10	5.2E+10	141.07	145.77	134.76	135.20	158.12	147.95	148.35	158.33	-29.76	-3.80	-23.71	-40.36
0.40	2.5E+10	9.5E+10	8.4E+09	9.2E+09	131.85	138.03	126.62	127.08	157.35	158.33	148.56	157.64	-44.50	-35.43	-38.45	-53.33
0.45	9.5E+08	3.9E+09	3.2E+08	3.5E+08	116.43	123.10	111.28	111.75	156.08	159.88	161.48	155.28	-69.21	-64.20	-87.61	-75.96
0.50	1.7E+08	9.9E+08	7.3E+07	8.1E+07	108.37	116.62	104.47	104.96	155.47	159.41	152.32	154.59	-82.20	-74.68	-83.51	-86.62
0.55	1.3E+07	1.2E+08	8.2E+06	9.2E+06	96.40	106.75	94.30	94.80	154.01	156.02	137.23	153.09	-100.54	-85.99	-74.92	-101.73
0.60	1.2E+06	1.1E+07	7.2E+05	8.1E+05	85.41	95.85	83.07	83.58	153.56	155.04	98.56	151.56	-118.94	-103.30	-27.04	-118.64
0.65	9.1E+04	9.0E+05	5.2E+04	5.8E+04	73.52	84.06	70.94	71.46	152.34	154.68	157.54	151.47	-137.56	-123.24	-151.14	-139.63
0.70	7.3E+03	7.6E+04	3.9E+03	4.4E+03	62.02	72.69	59.20	59.74	151.16	152.39	154.35	150.39	-155.56	-139.10	-166.05	-158.20
0.75	6.9E+02	7.5E+03	3.4E+02	3.9E+02	51.37	62.17	48.29	48.84	150.06	152.15	150.36	149.22	-172.24	-157.04	-178.14	-175.18
0.80	8.1E+01	9.5E+02	4.3E+01	4.3E+01	41.87	52.84	38.49	39.07	149.05	151.92	166.58	148.56	-187.05	-172.92	-223.53	-190.74
0.85	1.3E+01	1.6E+02	5.4E+00	6.2E+00	33.78	44.95	30.06	30.66	148.33	150.68	165.22	146.47	-199.92	-184.52	-235.88	-202.12
0.90	2.6E+00	3.7E+01	9.6E-01	1.1E+00	26.97	38.40	22.84	23.46	147.04	148.41	166.72	144.23	-209.55	-191.98	-251.10	-210.76
Avg.	-	-	-	-	109.43	116.85	104.88	105.36	158.24	158.70	156.51	158.15	-	-	-	-

\*Corresponding Author: Tirapote Rattana-amron  
E-mail address: tirapote@nanotec.or.th

**Table 1.** Thermodynamic parameters of extracted lignins according to four model-free methods (cont.)

$\alpha$	$A$ (s <sup>-1</sup> )				$AE$ (kJ/mol)				$AS$ (J/mol)			
	Friedman	FWO	KAS	Starink	Friedman	FWO	KAS	Starink	Friedman	FWO	KAS	Starink
<i>RS</i>												
0.10	2.8E+11	3.1E+12	5.3E+11	5.7E+11	134.80	145.46	137.61	137.92	169.04	168.67	168.94	168.93
0.15	1.8E+13	1.7E+14	2.5E+13	2.7E+13	153.25	163.41	154.83	155.17	168.42	168.12	168.38	168.36
0.20	6.0E+14	5.7E+15	7.9E+14	8.5E+14	169.02	179.08	170.20	170.56	167.95	167.68	167.92	167.91
0.25	2.8E+16	2.6E+17	3.5E+16	3.8E+16	186.26	196.26	187.19	187.55	164.12	163.89	167.46	164.09
0.30	1.3E+20	1.1E+21	1.5E+20	1.6E+20	223.98	233.94	224.68	225.05	161.70	161.60	166.58	161.73
0.35	5.2E+32	4.7E+33	5.6E+32	6.1E+32	355.31	365.32	355.62	356.01	164.36	164.23	167.36	164.35
0.40	3.2E+23	1.3E+24	1.4E+23	1.5E+23	259.31	265.75	255.60	256.00	165.89	165.77	165.96	165.95
0.45	2.3E+19	1.1E+20	1.1E+19	1.2E+19	216.43	223.53	212.86	213.29	163.06	163.00	166.84	163.21
0.50	1.9E+16	1.1E+17	8.7E+15	9.7E+15	184.54	192.16	180.98	181.43	164.29	164.22	164.51	164.50
0.55	3.0E+14	2.3E+15	1.7E+14	1.9E+14	165.86	175.01	163.36	163.83	168.05	167.79	168.12	168.10
0.60	1.2E+12	1.2E+13	8.2E+11	9.1E+11	141.41	151.66	139.54	140.02	168.81	168.47	168.87	166.19
0.65	2.2E+09	2.3E+10	1.3E+09	1.5E+09	113.30	123.70	111.06	111.56	166.71	169.45	169.96	169.94
0.70	1.3E+07	1.4E+08	7.0E+06	7.8E+06	90.57	101.13	87.98	88.51	167.60	167.11	171.05	167.71
0.75	2.2E+05	2.5E+06	1.1E+05	1.2E+05	72.87	83.60	69.93	70.48	168.71	168.09	168.90	168.87
0.80	8.0E+03	1.0E+05	3.7E+03	4.2E+03	58.65	69.57	55.34	55.91	172.93	172.15	173.20	173.15
0.85	5.8E+02	8.0E+03	2.4E+02	2.8E+02	47.50	58.65	43.81	44.40	173.89	172.93	174.25	174.19
0.90	6.0E+01	9.2E+02	2.2E+01	2.6E+01	38.01	49.45	33.88	34.50	174.88	173.71	175.38	175.31
Avg.	-	-	-	-	153.59	163.39	152.03	152.48	167.67	167.46	169.04	167.79
<i>CS</i>												
0.10	2.7E+10	3.0E+11	5.3E+10	5.7E+10	124.44	135.17	127.39	127.70	166.31	165.93	166.20	166.19
0.15	1.0E+12	1.0E+13	1.5E+12	1.6E+12	140.49	150.72	142.28	142.62	165.75	165.41	165.69	165.67
0.20	1.7E+14	1.7E+15	2.3E+14	2.5E+14	163.49	173.57	164.81	165.16	165.03	164.75	164.99	164.98
0.25	4.1E+17	3.8E+18	5.1E+17	5.5E+17	198.23	208.25	199.25	199.61	169.49	167.24	176.78	167.45
0.30	1.7E+30	8.4E+30	1.1E+30	1.2E+30	329.45	336.62	327.27	327.64	169.60	166.39	178.29	172.58
0.35	9.1E+31	1.2E+32	1.4E+31	1.5E+31	347.42	348.75	338.84	339.24	161.45	161.43	161.57	161.56
0.40	2.0E+23	2.0E+23	1.9E+22	2.1E+22	257.13	257.14	246.66	247.08	162.89	162.89	161.08	163.08
0.45	2.6E+22	4.9E+22	4.3E+21	4.7E+21	248.01	250.86	239.88	240.32	168.76	166.61	179.30	168.83
0.50	8.4E+16	1.7E+17	1.3E+16	1.4E+16	191.16	194.21	182.68	183.14	168.53	167.34	167.63	168.61
0.55	1.4E+13	3.9E+13	2.6E+12	2.9E+12	152.31	156.80	144.71	145.20	165.37	165.23	165.61	168.10
0.60	1.7E+11	8.8E+11	5.2E+10	5.8E+10	132.53	139.88	127.33	127.84	166.02	165.77	166.21	165.59
0.65	2.7E+09	2.3E+10	1.2E+09	1.4E+09	114.19	123.68	110.74	111.25	169.86	166.34	166.86	166.84
0.70	2.9E+07	3.3E+08	1.6E+07	1.8E+07	94.29	104.91	91.56	92.10	170.92	170.40	167.74	171.03
0.75	2.8E+05	3.4E+06	1.4E+05	1.6E+05	74.05	84.83	71.00	71.56	171.93	171.29	172.12	172.09
0.80	7.7E+03	9.9E+04	3.5E+03	4.0E+03	58.52	69.49	55.12	55.70	169.78	169.00	170.05	170.00
0.85	4.2E+02	5.9E+03	1.7E+02	2.0E+02	46.19	57.40	42.41	43.01	170.83	169.87	171.21	171.15
0.90	3.7E+01	5.9E+02	1.3E+01	1.5E+01	36.05	47.55	31.81	32.44	171.91	170.71	172.45	172.36
Avg.	-	-	-	-	159.29	167.05	155.52	155.98	167.91	166.86	169.04	168.01

\*Corresponding Author: Tirapote Rattana-amron  
E-mail address: tirapote@nanotec.or.th

The direction of the chemical process and the energy change throughout the formation of the activated complex are observed using the  $\Delta G$  value [34]. The variation of  $\Delta G$  at the conversion extent of 0.1-0.9 could be observed in Table 1. The average  $\Delta G$  for BG, CH, RS and CS obtained from four kinetic models were 163.61, 157.90, 167.99 and 167.96 kJ/mol, respectively. The greater  $\Delta G$  value of RS and CS pointed out that both lignins were more difficult to thermally convert than BG and CH. The positive magnitude of  $\Delta G$  is apparent at the thermal conversion of all soda lignins. It is evident from the results that the thermal oxidative degradation of lignin correlates with a non-spontaneous reaction [35].

According to the higher  $\Delta S$  degree, the substance is out of equilibrium with itself, resulting in an increasing degree of disorder in the system [36]. Results from Table 1 showed that thermal degradation soda lignin had a higher minus value of  $\Delta S$  at the end of conversion. This implies that the disordered degree of lignin is decreased after thermal oxidative degradation. In addition, the co-occurrence of both positive and negative  $\Delta S$  values can be observed during the process. This characteristic confirms that the specific thermal degradation processes of lignin have complex reactions [37].

#### 4. CONCLUSIONS

Based on the obtained data and kinetic and thermodynamic analyses, the following conclusions were created as follows:

1. Thermogravimetric analysis showed that the thermal degradation of lignin could be separated into three regimes, representing the moisture content, lignin degradation and decomposition of residue.
2. Friedman, FWO, KAS and Starink kinetic models were reliable for predicting the thermal stability of lignin at an acceptable level of accuracy.
3. Rice straw and corn stover had the highest thermal stability compared to the others.
4. Thermodynamic parameters ( $\Delta H$ ,  $\Delta G$  and  $\Delta S$ ) are obtained based on  $E$  values, revealing that thermal degradation of soda lignins is an endothermic reaction, which corresponds to a complex mechanism and degradation has never been spontaneous in nature.

#### Acknowledgement

The authors acknowledge the financial support of “Scholarship for the Development of High Quality Research Graduates in Science and Technology Petchra Pra Jom Klao Ph.D. Research Scholarship (KMUTT-NSTDA) from King Mongkut’s University of Technology Thonburi” and Program Management Unit for Human Resources & Institutional Development, Research and Innovation (PMU-B) contract number B42G670030. The authors are also thankful to NANOTEC, Thailand

#### References

- [1] Mujtaba, M., Fernandes Fraceto, L., Fazeli, M., Mukherjee, S., Savassa, S. M., Araujo de Medeiros, G., do Espírito Santo Pereira, A., Mancini, S. D., Lipponen, J., & Vilaplana, F. (2023). Lignocellulosic biomass from agricultural waste to the circular economy: a review with focus on biofuels, biocomposites and bioplastics. *Journal of Cleaner Production*, 402, 136815.
- [2] Khawkomol, S., Neamchan, R., Thongsamer, T., Vinitnantharat, S., Panpradit, B., Sohsalam, P., Werner, D., & Mroziak, W. (2021). Potential of Biochar Derived from Agricultural Residues for Sustainable Management. *Sustainability*, 13, 8147.
- [3] Lan, R., Eastham, S. D., Liu, T., Norford, L. K., & Barrett, S. R. H. (2022). Air quality impacts of crop residue burning in India and mitigation alternatives. *Nature Communications*, 13, 6537.
- [4] Awogbemi, O., & Kallon, D. V. V. (2022). Pretreatment techniques for agricultural waste. *Case Studies in Chemical and Environmental Engineering*, 6, 100229.
- [5] Lu, X., Gu, X., & Shi, Y. (2022). A review on lignin antioxidants: Their sources, isolations, antioxidant activities and various applications. *International Journal of Biological Macromolecules*, 210, 716-741.
- [6] Vyazovkin, S., & Wight, C. A. (1999). Model-free and model-fitting approaches to kinetic analysis of isothermal and nonisothermal data. *Thermochimica Acta*, 340-341, 53-68.

- [7] Luo, L., Guo, X., Zhang, Z., Meiyun, C., Rahman, M., Xingguang Zhang, W., & Cai, J. (2020). Insight into Pyrolysis Kinetics of Lignocellulosic Biomass: Isoconversional Kinetic Analysis by Modified Friedman Method. *Energy & Fuels*, 34, 4874–4881.
- [8] Emiola-Sadiq, T., Zhang, L., & Dalai, A. K. (2021). Thermal and Kinetic Studies on Biomass Degradation via Thermogravimetric Analysis: A Combination of Model-Fitting and Model-Free Approach. *ACS Omega*, 6, 22233-22247.
- [9] Gajera, B., Tyagi, U., Sarma, A. K., & Jha, M. K. (2022). Impact of torrefaction on thermal behavior of wheat straw and groundnut stalk biomass: Kinetic and thermodynamic study. *Fuel Communications*, 12, 100073.
- [10] Kumar, A., & Reddy, S. N. (2022). Study the catalytic effect on pyrolytic behavior, thermal kinetic and thermodynamic parameters of Ni/Ru/Fe-impregnated sugarcane bagasse via thermogravimetric analysis. *Industrial Crops and Products*, 178, 114564.
- [11] Wang, L., Lei, H., Liu, J., & Bu, Q. (2018). Thermal decomposition behavior and kinetics for pyrolysis and catalytic pyrolysis of Douglas fir. *RSC Advances*, 8, 2196-2202.
- [12] Friedman, H. L. (1964). Kinetics of thermal degradation of char-forming plastics from thermogravimetry. Application to a phenolic plastic. *Journal of Polymer Science Part C: Polymer Symposia*, 6, 183-195.
- [13] Ozawa, T. (1965). A New Method of Analyzing Thermogravimetric Data. *Bulletin of The Chemical Society of Japan - BULL CHEM SOC JPN*, 38, 1881-1886.
- [14] Flynn, J. H., & Wall, L. A. (1966). A quick, direct method for the determination of activation energy from thermogravimetric data. *Journal of Polymer Science Part B: Polymer Letters*, 4, 323-328.
- [15] Çepelioğullar, Ö., Haykırı-Açma, H., & Yaman, S. (2016). Kinetic modelling of RDF pyrolysis: Model-fitting and model-free approaches. *Waste Management*, 48, 275-284.
- [16] Doyle, C. D. (1962). Estimating isothermal life from thermogravimetric data. *Journal of Applied Polymer Science*, 6, 639-642.
- [17] Kissinger, H. E. (1957). Reaction Kinetics in Differential Thermal Analysis. *Analytical Chemistry*, 29, 1702-1706.
- [18] Hu, Y., Wang, Z., Cheng, X., & Ma, C. (2018). Non-isothermal TGA study on the combustion reaction kinetics and mechanism of low-rank coal char. *RSC Advances*, 8, 22909-22916.
- [19] Huang, H., Liu, J., Liu, H., Evrendilek, F., & Buyukada, M. (2020). Pyrolysis of water hyacinth biomass parts: Bioenergy, gas emissions, and by-products using TG-FTIR and Py-GC/MS analyses. *Energy Conversion and Management*, 207, 112552.
- [20] Starink, M. J. (2003). The determination of activation energy from linear heating rate experiments: a comparison of the accuracy of isoconversion methods. *Thermochimica Acta*, 404, 163-176.
- [21] Zou, H., Evrendilek, F., Liu, J., & Buyukada, M. (2019). Combustion behaviors of pileus and stipe parts of *Lentinus edodes* using thermogravimetric-mass spectrometry and Fourier transform infrared spectroscopy analyses: Thermal conversion, kinetic, thermodynamic, gas emission and optimization analyses. *Bioresource Technology*, 288, 121481.
- [22] Bertini, F., Canetti, M., Cacciamani, A., Elegir, G., Orlandi, M., & Zoia, L. (2012). Effect of ligno-derivatives on thermal properties and degradation behavior of poly(3-hydroxybutyrate)-based biocomposites. *Polymer Degradation and Stability*, 97, 1979-1987.
- [23] Xiong, S. J., Zhou, S. J., Wang, H. H., Wang, H. M., Yu, S., Zheng, L., & Yuan, T. Q. (2022). Fractionation of technical lignin and its application on the lignin poly-(butylene adipate-co-terephthalate) bio-composites. *International Journal of Biological Macromolecules*, 209, 1065-1074.
- [24] Nazimudheen, G., Sekhar, N. C., Sunny, A., Kallingal, A., & B, H. (2021). Physiochemical characterization and thermal kinetics of lignin recovered from sustainable agrowaste for bioenergy applications. *International Journal of Hydrogen Energy*, 46, 4798-4807.
- [25] Yeo, J. Y., Chin, B. L. F., Tan, J. K., & Loh, Y. S. (2019). Comparative studies on the pyrolysis of cellulose, hemicellulose, and lignin based on combined kinetics. *Journal of the Energy Institute*, 92, 27-37.
- [26] Yang, J., Feng, Z., Gao, Q., Ni, L., Hou, Y., He, Y., & Liu, Z. (2021). Ash thermochemical behaviors of bamboo lignin from kraft pulping: Influence of washing process. *Renewable Energy*, 174, 178-187.
- [27] Chen, D., Zhou, J., & Zhang, Q. (2014). Effects of heating rate on slow pyrolysis behavior, kinetic parameters and products properties of moso bamboo. *Bioresource Technology*, 169, 313-319.
- [28] Mumbach, G. D., Alves, J. L. F., da Silva, J. C. G., Domenico, M. D., Arias, S., Pacheco, J. G. A., Marangoni, C., Machado, R. A. F., & Bolzan, A. (2022). Prospecting pecan nutshell pyrolysis as a source of bioenergy and bio-based chemicals using multicomponent kinetic modeling, thermodynamic parameters estimation, and Py-GC/MS analysis. *Renewable and Sustainable Energy Reviews*, 153, 111753.
- [29] Zhang, S., & Wang, F. (2022). Effect of interactions during co-combustion of organic hazardous wastes on thermal characteristics, kinetics, and pollutant emissions. *Journal of Hazardous Materials*, 423, 127209.
- [30] Qiao, Y., Wang, B., Ji, Y., Xu, F., Zong, P., Zhang, J., & Tian, Y. (2019). Thermal decomposition of castor oil, corn starch, soy protein, lignin, xylan, and cellulose during fast pyrolysis. *Bioresource Technology*, 278, 287-295.

- [31] Anca-Couce, A., Mehrabian, R., Scharler, R., & Obernberger, I. (2014). Kinetic scheme of biomass pyrolysis considering secondary charring reactions. *Energy Conversion and Management*, 87, 687-696.
- [32] Turmanova, S. (2008). Non-isothermal degradation kinetics of filled with rice husk ash polypropylene composites. *Express Polymer Letters*, 2, 133-146.
- [33] Georgieva, I., Mulder, C. L., & Wierdsma, A. (2012). Patients' preference and experiences of forced medication and seclusion. *Psychiatric Quarterly*, 83, 1-13.
- [34] Saffe, A., Fernandez, A., Echegaray, M., Mazza, G., & Rodriguez, R. (2019). Pyrolysis kinetics of regional agro-industrial wastes using isoconversional methods. *Biofuels*, 10, 245-257.
- [35] Pawar, A., Panwar, N. L., Jain, S., Jain, N. K., & Gupta, T. (2023). Thermal degradation of coconut husk waste biomass under non-isothermal condition. *Biomass Conversion and Biorefinery*, 13, 7613-7622.
- [36] Bahú, J. O., de Oliveira, R. A., De Souza, L. M. A., Rivera, E. C., Felisbino, R. F., Maciel Filho, R., & Tovar, L. P. (2022). Kinetic study of thermal decomposition of sugarcane bagasse pseudo-components at typical pretreatment conditions: Simulations of opportunities towards the establishment of a feasible primary biorefining. *Cleaner Chemical Engineering*, 4, 100074.
- [37] Ahmad, M. S., Mehmood, M. A., Liu, C.-G., Tawab, A., Bai, F.-W., Sakdaronnarong, C., Xu, J., Rahimuddin, S. A., & Gull, M. (2018). Bioenergy potential of *Wolffia arrhiza* appraised through pyrolysis, kinetics, thermodynamics parameters and TG-FTIR-MS study of the evolved gases. *Bioresource Technology*, 253, 297-303.